Effective deterministic models for chaotic dynamics perturbed by noise

Lars Jaeger* and Holger Kantz
Max-Planck-Institut für Physik Komplexer Systeme, Bayreuther Strasse 40, D-01187 Dresden, Germany
(Received 18 December 1996)

The possibility of representing deterministic chaotic systems perturbed by interactive noise by a purely deterministic process with observational noise is discussed. We investigate the shadowing of pseudotrajectories of a given dynamics by trajectories of a different (nearby) dynamics. A method of constructing the effective deterministic model from observed data is presented and the relevance of this model to the observed data is verified by several quantities. [S1063-651X(97)08405-5]

PACS number(s): 05.45.+b

I. INTRODUCTION

In every discussion about the relevance of the theory of nonlinear dynamical systems and ergodic theory of strange measures for realistic physical situations, the influence of noise is an important issue. In experiments and in some sense also in computer simulations [1] one does not observe the time evolution of a dynamical system in the mathematical sense, but instead a nonlinear stochastic process, where, however, the stochastic component is small in comparison to the other terms. This *dynamical* or *interactive* noise interferes with the deterministic part of the dynamics and, as many studies show, can have considerable effects, much more severe than just reducing the information about the current state of the system as in the case of *measurement* or *observational* noise.

This has implications for both principal reasons and practical considerations, in particular in nonlinear time-series analysis, where one tries to extract information about the underlying system from experimental observations. The standard tools of treating noise in chaotic data assume the existence of a nearby (shadowing) clean trajectory fulfilling the underlying deterministic dynamics exactly. Based on this assumption, sophisticated noise reduction schemes were developed [3–5]. In [6] it was shown that it is possible to estimate the exact dynamics of chaotic time series contaminated by large-amplitude observational noise using a cost function that constructs locally shadowing pieces of trajectories. Unfortunately, in the presence of *dynamical* noise, only for a very limited class of systems are the problems as simple to treat: In hyperbolic systems the shadowing lemma [7] holds and a deterministic trajectory close to the noisy one exists such that the problem is basically reduced to treating measurement noise. Unfortunately, hyperbolicity is a property that is supposed never present in ''real world'' systems, so a clean shadowing trajectory of the original noise-free dynamics generally does not exist. The results for many procedures of nonlinear time-series analysis therefore become questionable in the presence of dynamical noise. This paper addresses dynamical noise. Throughout the paper we will consider systems of a Langevin type

$$\dot{\mathbf{x}}(t)=\mathbf{f}(\mathbf{x}(t))+\boldsymbol{\xi}(t) \quad \text{(flow)}, \tag{1}$$

$$\mathbf{x}_{n+1}=\mathbf{F}(\mathbf{x}_n)+\boldsymbol{\xi}_n \quad \text{(map)},$$

where $\boldsymbol{\xi}(t)$ and $\boldsymbol{\xi}_n$ define some stochastic processes, in our case simple white noise. We consider the effects of noise in the zero-noise limit, i.e., the reference system remains the deterministic dynamics.

If the deterministic dynamics f is nonhyperbolic, it is impossible to shadow a noisy trajectory by an exact solution of f. This is already visible in Fig. 1, where we observe the noise-induced attractor prolongations investigated in detail in [8]. Obviously, there cannot be any shadowing if the noisy attractor spreads out into regions that are not part of the clean attractor. In this paper we shall construct dynamical systems $\tilde{f}$ that are close to f and whose solutions are able to shadow the solutions of the noisy system much better (parameter shadowing). This is demonstrated by a comparison of characteristic quantities such as the attractor geometry and Lyapunov exponents for the effective dynamics $\tilde{f}$ and the original dynamics f. Moreover, starting from a deterministic time evolution, we shall construct pseudo-orbits that still violate determinism, but in a much weaker way than the given noisy orbits, and are close to them. Again it will turn out that a suitably constructed nearby deterministic dynamics is superior to f when used in this construction.

As shadowing with the original dynamics turns out to be impossible, we introduce (motivated by the work in [9]) the concept of ''parameter shadowing,'' i.e., the construction of a trajectory that fulfills a nearby dynamics and evolves in the neighborhood of the noisy trajectory. This paper is devoted to two different aspects. Our first concern is the construction of such an effective deterministic dynamics that allows for shadowing. Using the method introduced in [6] (and to be briefly reviewed below), we obtain $\tilde{f}$, which, by construction, is the optimal dynamics for finite-time shadowing. Moreover, we will be able to construct a different pseudotrajectory both closer to determinism and closer to the observed data than any trajectory obtained with the help of f. Noise reduction via minimization of the dynamical error [5] and the breakdown of shadowing at homoclinic tangencies (HTs) will be discussed in Sec. II, while the construction of an effective dynamics $\tilde{f}$ will be discussed in Sec. III. Second, in

*Electronic address: jaeger@mpipks-dresden.mpg.de

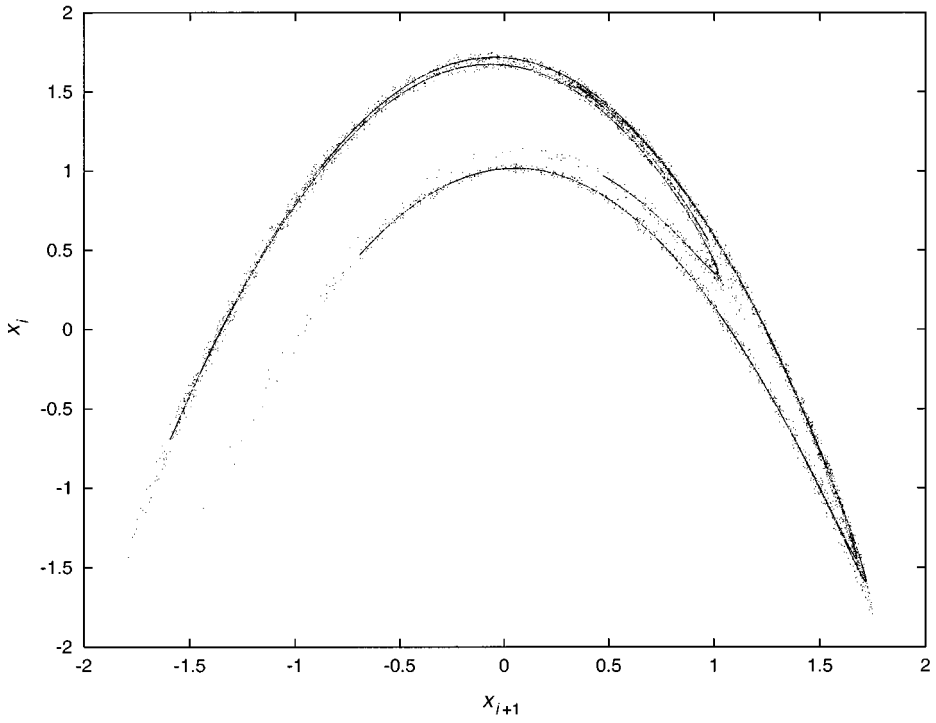

FIG. 1. Hénon attractor, clean and with 3% dynamical noise (uniformly distributed and white). Note the attractor prolongation exceeding the noise level by an order of magnitude at homoclinic tangencies.

order to give quantitative criteria for the relevance of $\tilde{f}$ for the noisy system, we want to give an analysis of the possible effects and associated difficulties of dynamical noise in chaotic systems. We will apply different appropriate measures and characterizations of the features of the noisy system compared with the purely deterministic one. A comparison of these features obtained for the noisy attractor with those of the attractor of $\tilde{f}$ gives a very accurate correspondence in contrast to what we obtain with the original dynamics f. This will be treated in Sec. IV, with a numerical investigation in Sec. V, where we exemplify our concepts for the Hénon system as well as for an experimental data set.

Let us briefly make a comment concerning the interpretation of real world data. In the presence of dynamical noise the question for the ''correct model'' is somehow ambiguous and the goal of modeling is less well described than in the case of mere measurement noise. The optimal model would yield the deterministic part of the dynamical equations, the details of the noise process (distribution, temporal correlations, and higher moments), and the interaction between them. It is obvious that this is generally too ambitious, and from a more practical point of view one might ask for a deterministic dynamical system that can reproduce the observed attractor with its geometrical and topological features. So, in the presence of dynamical noise the aim of constructing the ''original'' dynamics that models the noise-free data can be of secondary interest when we want to encounter the noise-induced effects in our model as well.

II. DYNAMICAL NOISE AND SHADOWING

A. Dynamical noise and homoclinic tangencies

Noise in dynamical systems leads to so-called pseudotrajectories $\{\mathbf{x}_i\}$ with respect to the underlying dynamics f: For $\alpha>0$ an (α) pseudotrajectory is a sequence $\{\mathbf{x}_i\}_{i=-\infty}^{\infty}$ of points $\mathbf{x}_i$ such that $||\mathbf{f}(\mathbf{x}_i)-\mathbf{x}_{i+1}||<\alpha$. The size of α or, equivalently, the dynamical error E_{dyn}: $=\sqrt{(1/N)\Sigma_i[\mathbf{x}_{i+1}-\mathbf{f}(\mathbf{x}_i)]^2}$ (N is the length of the pseudotrajectory) gives a measure of how close this pseudotrajectory is to determinism. Much work in the past few years has been dedicated to the construction of a deterministic shadowing orbit of the pseudotrajectory [1,4]. For dynamical noise these methods rely on the shadowing theorem [7], which guarantees the existence of an orbit of the noise-free system that shadows the pseudo-orbit in hyperbolic systems corrupted by bounded noise. All the construction methods therefore require the hyperbolicity of the system f. In the presence of HTs, tangencies between the stable and unstable manifolds, these schemes neccessarily fail since the existence of a lower bound $\epsilon>0$ for the angle between the stable and the unstable manifold is essential [1,7]. In fact, at HTs the trajectory is generally driven away from the neighborhood of the attractor: This was systematically investigated in [8] and shall only be discussed very briefly here.

At a HT there is no clear factorization of the tangential space into contracting and expanding directions possible. A perturbation cannot be driven along the stable manifold back to the attractor after a small number of iterations as in the hyperbolic case. Instead, due to the tangential structure of the stable and unstable manifolds at a HT, it is driven away from the neighborhood of the attractor. The most expanding direction in the tangential space of a HT is perpendicular to the attractor itself. Through this mechanism noise can be amplified by orders of magnitude. Only through the folding due to the nonlinearity does the trajectory return to the neighborhood of the attractor after a certain number of iterations.

There is evidently no shadowing possible if this mechanism, which creates the noise-induced prolongation of the attractor easily observable in many nonhyperbolic systems in the presence of dynamical noise, applies. The question now is the following: Is there a modified dynamics $\tilde{f}$ that is fulfilled by a deterministic trajectory $\{\tilde{\mathbf{x}}\}_i$ shadowing the

TABLE I. Minimum of the one-step prediction error (3) for dynamical noise and measurement noise on the Hénon system with $a=1.38$ and $b=0.27$ on pseudo-orbits found by minimizing Eqs. (3) and (4) with respect to x_i. N was chosen to be 5000.

Noise level	0.005	0.01	0.015	0.02	0.025	0.03	0.035
Dynamical noise (units of 10^{-4})	4.5	11.28	18.43	24.22	33.03	41.59	47.41
Measurement noise (units of 10^{-4})	0.0014	0.0022	0.0025	0.0026	0.0034	0.0045	0.0046

pseudotrajectory such that the noisy trajectory can be essentially described by a deterministic trajectory plus observational noise? This would be represented by

$$\tilde{\mathbf{x}}_{i+1}=\tilde{f}(\tilde{\mathbf{x}}_i), \qquad \mathbf{x}_i=\tilde{\mathbf{x}}_i+\tilde{\boldsymbol{\xi}}. \tag{2}$$

Here $\tilde{\boldsymbol{\xi}}$ indicates some ''pseudonoise'' describing the distance between the noisy and the shadowing trajectory. Following [9], we call this modified version of shadowing parameter shadowing. There are two steps to be taken in order to approach this question. We first have to construct the dynamics $\tilde{f}$ underlying the shadowing orbit. Second, we have to construct the shadowing orbit itself. It will turn out that both concepts are intimately related.

We are not able to prove parameter shadowing in mathematical terms (for one-dimensional maps see [9] for a rigorous approach). Instead, we present a way to construct an approximate solution: We derive a dynamics that describes the features of the noisy system (see Sec. IV) much better than the original dynamics. This allows us to construct short segments of shadowing trajectories for $\tilde{f}$ even in the vicinity of HTs. Alternatively, we derive a pseudotrajectory of $\tilde{f}$ that is much closer to determinism, i.e., has much smaller E_{dyn}, compared to the same construction for the original dynamics. We are thus not neccessarily dealing with a deterministic (referring to the modified dynamics) shadowing trajectory, but rather with a different pseudotrajectory with much smaller dynamical error than anyone constructed with the original dynamics.

B. Noise reduction based on shadowing

The construction of an exactly shadowing orbit remains difficult, if not impossible, even in the case of pure observational noise (where an exactly shadowing orbit for the original dynamics trivially exists). In [4] a method based on singular value decomposition and manifold decomposition is introduced, and in [1] a technique that uses Bowen's construction in the proof of the shadowing theorem [7] is presented. Both methods fail at HTs (in the case of measurement noise already). In the spirit of our aim we are here looking for a method that produces a shadowing pseudotrajectory as deterministic as possible. Such a method was introduced in [5]. Given the dynamics $\tilde{f}$ in delay embedding space [10], the cost function

$$L=\frac{1}{N}\sum_{i=1}^{N}[x_{i+1}-\tilde{f}(\mathbf{x}_i)]^2 \tag{3}$$

is minimized with respect to the points $\{x_i\}$ by gradient descent methods starting with the noisy points as initial conditions. Conjugate gradient methods have proven to be very robust and efficient for our purpose. In the case of measurement noise $\tilde{f}$ is simply the original dynamics (assumed to be known or very accurately estimated), and if unique, the solution reduces L to zero (there is more than one solution to the minimization problem in most cases; see [5]). For dynamical noise, though, the minimum of Eq. (3) with the original dynamics is considerably large, which is due to a huge deviation from deterministic behavior at HTs. Table I and Fig. 2 show this very clearly. In Table I we show the minimum of Eq. (3) for the Hénon dynamics [11]

$$x_{n+1}=a-x_n^2+bx_{n-1}, \tag{4}$$

with $a=1.38$ and $b=0.27$ perturbed with dynamical noise and measurement noise, respectively. In Fig. 2, the value of $E^i_{\mathrm{dyn}}=|x_{i+1}-f(\mathbf{x}_i)|$ for each point of the noise-reduced trajectory is given for measurement noise and for dynamical noise, respectively. The noise level η throughout this paper is given in percent of the standard deviation of the signal (rms): $\eta=\sigma_{\mathrm{noise}}/\sigma_{\mathrm{signal}}$. While E^i_{dyn} reduces to machine precision for measurement noise, it is observable that large values of E^i_{dyn} in the case of dynamical noise occur at certain times. These correspond to the trajectory being near primary HTs [8,12] as we explicitly checked by plotting the corresponding points on the attractor.

For the remainder of this paper, two problems related to the noise reduction scheme introduced in [5] are relevant. First, HTs also have an effect on the noise reduction for measurement noise by making the minimum of Eq. (3) not unique such that a different shadowing trajectory can exist besides the original deterministic one [5]. The distance of the noise-reduced trajectory from the original clean trajectory can therefore still remain considerably large while E_{dyn} is reduced to machine precision. Second, all noise-reduction schemes based on shadowing (globally or locally) require the knowledge of the underlying deterministic dynamics (or at least a very accurate estimate of it). A poor fit of the dynamics makes the noise-reduction scheme perform poorly too. The performance of noise reduction can thus give a measure for the accuracy of the fit of the dynamics.

In Fig. 3 we show the errors $E_{\mathrm{dyn}}=\sqrt{(1/N)\Sigma_{i=1}^{N}(E^i_{\mathrm{dyn}})^2}$ and $E_0=\sqrt{(1/N)\Sigma_{i=1}^{N}(x_i-y_i)^2}$ for a noise-reduced trajectory $\{x_i\}$ (from originally 2% measurement noise, $\{y_i\}$ denotes the corresponding clean trajectory, which, of course, can only be defined in the case of measurement noise), where different dynamics $\tilde{f}$ were used: We vary the paramater a in Eq. (4) between $a=1.34$ and $a=1.42$ (where $a=1.38$ is the original parameter). Additionally, we show the average cor-

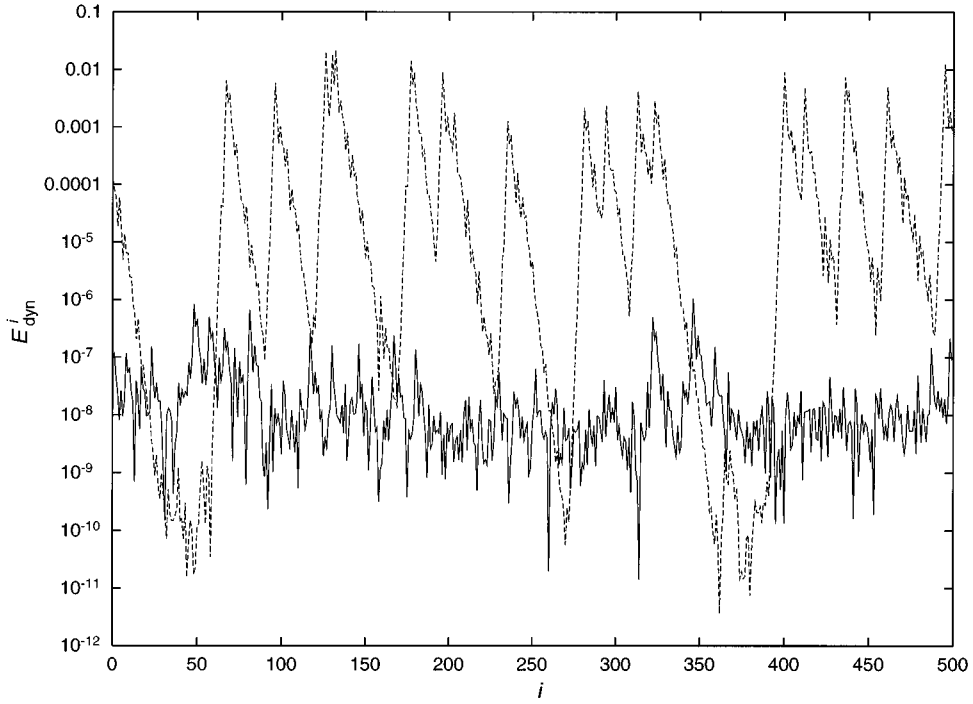

FIG. 2. Individual one-step prediction errors $E^i_{\rm dyn}=|y_{i+1}-f(\mathbf{y}_i)|$ after noise reduction with Eq. (3) using the dynamics (4) at different times i for 3.5% measurement noise (lower curve) and dynamical noise on the Hénon system with $a=1.38$ and $b=0.27$.

rection of the original noisy trajectory $\{s_i\}$: $E_d=\sqrt{(1/N)\Sigma_{i=1}^{N}(s_i-x_i)^2}$. A large average correction E_d exceeding the noise level indicates bad performance. A poor estimate for the dynamics yields very high $E_{\rm dyn}$ and/or E_0, E_d. Conversely, we call the capacity of the dynamics f to allow for shadowing of a given noisy trajectory high if both $E_{\rm dyn}$ and E_d are small.

For the case of dynamical noise we will show that the original dynamics is such a poorly performing dynamics for noise reduction in the same sense: We will obtain comparably bad values of $E_{\rm dyn}$ and E_d. The construction of an effective deterministic ''nearby dynamics'' in Sec. IV leads to noise-reduced trajectories whose violation of determinism is about one order of magnitude smaller than the original dynamics shown in Table I and Fig. 2.

III. LOCAL SHADOWING AND THE RECONSTRUCTION OF THE EFFECTIVE DYNAMICS

A. The effective dynamics

The minimization problem introduced in [6] for the unbiased reconstruction of the dynamics in the presence of large-amplitude measurement noise turns out to lead to the desired effective model we are looking for. We are solving the local

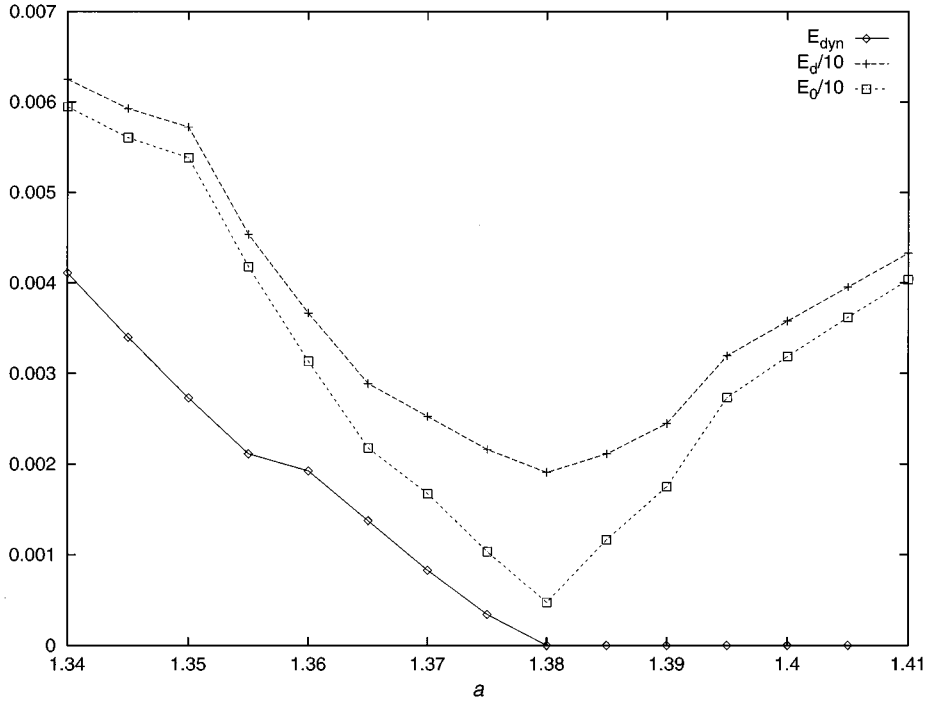

FIG. 3. $E_{\rm dyn}$, E_0, and E_d for a cleaned trajectory (from 2% measurement noise) of the Hénon system (4), where different dynamics were used for the noise reduction (3). The parameter a is varied from $a=1.34$ to $a=1.42$.

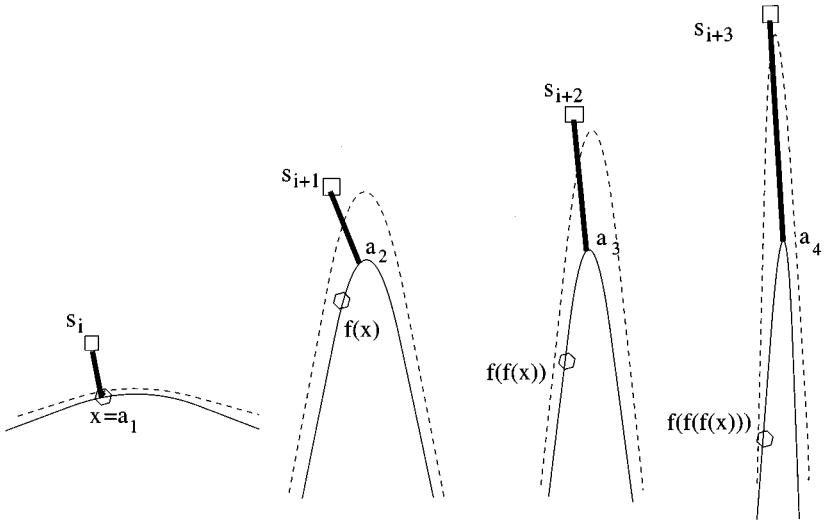

FIG. 4. Loss of shadowing at HTs in the case of dynamical noise [8]. The continuous curves represent parts of the attractor of the true dynamics or a dynamics obtained using a cost function that does not use local shadowing. Three points of the noisy trajectory and their base points for $k=1$ are shown (the time order is from left to right). The base points are far away from the images of previous base points (given by a hexagon) as the noisy points (indicated by a square) are driven away from the attractor. There are no image points of a constructed base point in the neighborhood of the noisy point. The dashed graph represents the attractor of the modified effective dynamics: It enables local shadowing of the noisy trajectory. In order to obtain this effective dynamics a multistep prediction error ($k>1$) in Eq. (5) has to be used.

shadowing problem, and we obtain the optimal effective model for the locally shadowing pieces of trajectory. A suitable combination of different components in the resulting vectors yields the global pseudo-orbit. We recall our method in the following: We are searching for deterministic pieces of a trajectory (for k time steps) obeying the dynamics $\tilde{f}$, which are at the same time close to the observed data over k time steps. Thus, for each delay vector $\mathbf{s}_i$ we introduce a point $\mathbf{a}_i$ and its k images under the dynamics $\tilde{f}$. Then the contribution of a given single delay vector $\mathbf{s}_i$ to the new cost function is the sum of the k Euclidean distances between k pairs of $(m+1)$-dimensional vectors: The first pair is $(\mathbf{s}_i, s_{i+1})$ and the vector $(\mathbf{a}_i, \tilde{f}(\mathbf{a}_i))$, the next $k-1$ pairs are formed by the successive images of these two vectors, where the images of the noisy vector $(\mathbf{s}_i, s_{i+1})$ are just read off from the noisy input data, and the images of $(\mathbf{a}_i, \tilde{f}(\mathbf{a}_i))$ are constructed with the dynamics $\tilde{f}$. Finally, $\mathbf{a}_i$ is defined by the fact that it minimizes the sum of these k distances or, in other words, minimizes the accumulated k-step Euclidean prediction error. The points $\mathbf{a}_i$ are called base points in the following and represent the optimal shadowing piece of a trajectory with dynamics $\tilde{f}$. We are looking for $\tilde{f}$ such that these shadowing orbits are optimally close to the observed data. The cost function thus reads

$$S^2=\sum_{i=m}^{T-n}\sum_{j=1}^{k}|(s_{i+j-m},\ldots,s_{i+j})-(a_{i,j-m},\ldots,a_{i,j})|^2, \tag{5}$$

which has to be minimized with respect to the $\mathbf{a}_i$ and the parameters in $\tilde{f}$.

The numerical implementation of this cost function for different *Ansätze* of the function f is in detail discussed in [6]. It was shown that this methods works very well in the case of pure measurement noise, where a shadowing trajectory of the original dynamics evidently exists, and the true underlying original dynamics could be obtained to very high accuracy. The multistep cost function avoids the problem of mutual inconsistency between subsequent base points encountered if one uses only a one-step prediction error cost function.

Due to the lack of a shadowing trajectory of the original dynamics in the case of dynamical noise we observe a strong form of what we phrased ''mutual inconsistency'' in [6] that cannot be overcome on using the original dynamics. For $k=1$ in Eq. (5) the image of a base point $\mathbf{a}_i$ of a point $\mathbf{s}_i$ is generally not close to the base points $\mathbf{a}_{i+j}$ of the next points $\mathbf{s}_{i+j}$ of the pseudotrajectory. Especially at HTs the mechanism described above and in [8] induces the loss of the shadowing possibility, which is explained in Fig. 4. The use of the standard cost function (3) (with minimization with respect to the parameters in $\tilde{f}$) or using $k\approx 1$ in Eq. (5) is not sensitive to this mutual inconsistency as local shadowing is not used. By calculating the optimal effective dynamics using the cost function (5) with sufficiently large k we suppress this mutual inconsistency: The resulting dynamics $\tilde{f}$ (schematically given in Fig. 4 by a dashed line) by construction leads to local shadowing for the noisy trajectory also at HTs. The base points $\{\mathbf{a}_i\}$ appropriately weighted over the different components serve well for a noise-reduced trajectory. Thus we obtain both the effective deterministic dynamics and the approximate shadowing orbit. In principle, one should choose the number of steps k as large as possible. The higher k is chosen the better our construction of an ''effective'' dynamics for the noisy trajectory is. If we were able to find an initial vector $\mathbf{a}_m$ and a function f such that the iterates of $\mathbf{a}_m$ remain close to the observed data for all the next $T-m$ steps, we would have solved the problem in the optimal way: We would know a shadowing clean trajectory for all our noisy observations. Due to the sensitive dependence

on initial conditions, this is numerically not achievable, and in practice we are able to proceed until $k \approx 15$. For most systems, though, for $k \approx 15$ the divergence of trajectories initially within the noise level will reach the length scale of the entire attractor.

B. Increased parameter shadowing

In [9] it was rigorously shown that one-dimensional maps can allow increased parameter shadowing in specific parameter regimes: For a given pseudotrajectory of a dynamics f_a there exists a $\delta > 0$ such that there exists a shadowing trajectory evolving after $f_{a+\delta}$, where it is assumed that the Kolmogorov-Sinai (KS) entropy of the map increases monotonically in a. The increase of the parameter for the tent map and the logistic equation is then related to the increase of the entropy under perturbation with noise. In this section we want to relate our work to these results. Our method is not restricted to a specific class of systems, but, of course, applicable to the one-dimensional maps considered in [9]. Our quantitative results are in full agreement with their qualitative predictions. Choosing the *Ansatz* of a quadratic polynomial $f_a(x) = 1 - ax^2$ with only a as a parameter and applying the cost function (5) for a fit, we obtain increasing parameters a for the effective deterministic dynamics; see Fig. 5: Complementing the results in [9] our methods thus yields quantitative results: We chose $a = 1.8$ for the deterministic map and construct the effective dynamics for different k in Eq. (5) and noise levels. The effective parameter a describing the effective dynamics increases with k and converges against an effective a that can be considered as the optimal increased shadowing parameter. In order to show the relevance of these effective parameters we construct pseudotrajectories using the new parameters and compare the result to the old parameters (Fig. 5): The capacity of $\tilde{f}_a$ for shadowing increases drastically.

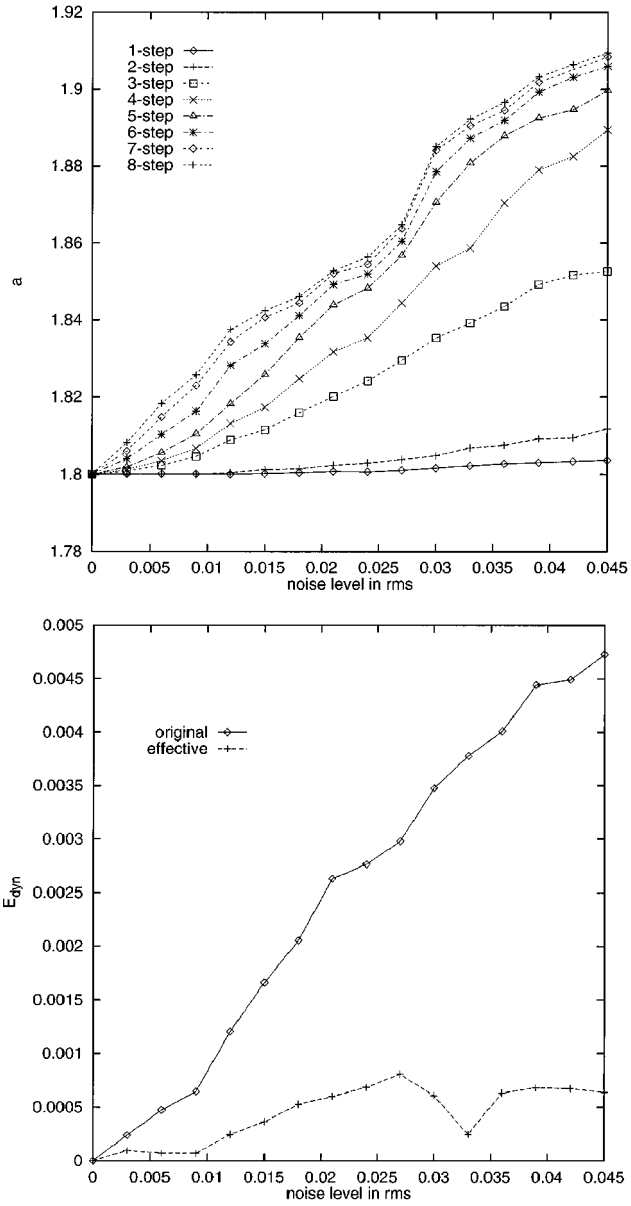

FIG. 5. Logistic map $x_{n+1} = 1 - 1.8x_n^2$ with noise. The dynamics was reconstructed according to Eq. (5) for different k using the quadratic ansatz $f_a(x) = 1 - ax^2$. The parameter a versus the noise level in rms is shown. Below we show the obtained E_{dyn} after noise reduction with the original dynamics $x_{n+1} = 1 - 1.8x_n^2$ and the effective dynamics with a value of a obtained for $k = 8$.

IV. CHARACTERIZATION OF NOISY SYSTEMS

The presence of noise changes the invariant features of the system. Exactly speaking, dimensions, entropies, and Lyapunov exponents defined in the standard way become meaningless since on the small scales the noise process dominates and they become infinite. If the noise level is small enough, though, we are still able to observe the characteristic scaling properties on larger scales such that effective Lyapunov exponents can be defined. These values can differ considerably from the deterministic values.

In this section we want to develop some measures in order to compare the effective dynamics $\tilde{f}$ constructed in Sec. III to the original dynamics f to show quantitatively the relevance of $\tilde{f}$ for the modeling of the noisy data. They will be used for model verification in Sec. V.

A. Cross correlations

The scaling range of the standard correlation dimension [13] $D_2(\epsilon) \approx (\partial / \partial \ln \epsilon) \ln \sum_{i,j \neq i}^{T} \Theta(\epsilon - |\mathbf{x}_i - \mathbf{x}_j|) \approx \text{const}$ is limited to large scales in the presence of noise. The standard correlation sum is not very useful in the case of dynamical noise, as the noise acts on different length scales (noise-induced attractor deformation [8]). Another question is how comparable the noisy attractor is with the original attractor of the deterministic system after the deformations or prolongations occurring due to noise [8]. A quantitative comparison of the shape of two fractal attractors can be made by the cross correlation sum. First we reconstruct the attractor by delay embedding with dimension m. A measure for the deviation of the noisy attractor from the clean attractor is then given in [14], to which we refer for more details: Computing the cross correlation sum

$$C_{XY}(\epsilon) = \frac{1}{|X||Y|} \sum_{i}^{|X|} \sum_{j}^{|Y|} \Theta(\epsilon - ||\mathbf{x}_i - \mathbf{y}_j||) \qquad (6)$$

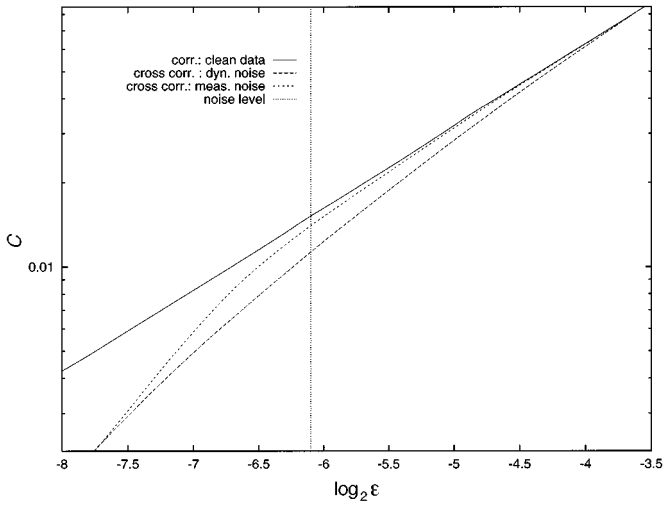

FIG. 6. Cross correlation sums C between clean and noisy Hénon attractor (4) with 2% white uniform noise for dynamical noise and measurement noise. The length scale is given in a dyadic logarithm. The vertical line gives the noise level.

between the set X of clean data points $\mathbf{x}_i$ and the set Y of noisy points $\mathbf{y}_j$, the differences between the attractors become observable below a critical ϵ_c. Precisely, after defining a tolerance ρ, ϵ_c is defined as follows: for $\epsilon<\epsilon_c$,

$$|\ln C_{XX}-\ln C_{XY}|\leqslant\rho, \quad |\ln C_{YY}-\ln C_{XY}|\leqslant\rho,$$

and for $\epsilon\geqslant\epsilon_c$,

$$|\ln C_{XX}-\ln C_{XY}|>\rho \quad \text{or} \quad |\ln C_{YY}-\ln C_{XY}|>\rho. \qquad (7)$$

In the case of measurement noise this ϵ_c is again determined by the noise level [14]. The specific effects of dynamical noise on different length scales can be very well observed in the cross correlation with the clean data exemplified in Fig. 6 for the Hénon system: The curve for measurement noise characterizes a distinct ϵ_c corresponding to the noise level, while the curve for dynamical noise shows an ϵ_c that is an order of magnitude larger than the noise level. This is a signature of the noise-induced attractor deformation described above and in [8]. A dynamics that describes the noisy data more appropriately is expected to yield an attractor in better correspondence with the noisy one: The attractor should form a good ''skeleton'' for the noisy atractor (see Figs. 1 and 9), such that the cross orrelation diverges from the autocorrelation (solid line) at smaller ϵ.

B. Lyapunov exponents

The degree of chaos in noisy systems can be measured by considering the rate of divergence of two initially close trajectories under the same realization of noise. Mathematically there exists a well-defined concept of Lyapunov exponents in what is called stochastic dynamical systems [15,16]. The maximal Lyapunov exponent is thus defined by

$$\lambda=\lim_{T\to\infty}\frac{1}{T}\ln\left(\left|\prod_{i=1}^{T} Df(\mathbf{x}_i)\mathbf{u}_0\right|\right), \qquad (8)$$

where $\{\mathbf{x}_i\}$ is the noisy trajectory, for almost all $\mathbf{u}_0$. This is a clear mathematical definition, but it can lead to a severe misinterpretation of the effects of noise (e.g., the claim of noise-induced order in the logistic map [17]). In applications to noisy systems one has to make the unrealistic assumption that neighboring trajectories are subject to the identical noise realization, such that the exponent given by Eq. (8) can never be determined from experimental data. In [18] a more natural indicator of chaos in noisy systems is introduced considering the rate of separation of nearby trajectories under different realizations of noise that corresponds exactly to what one calculates when determining the Lyapunov exponent using

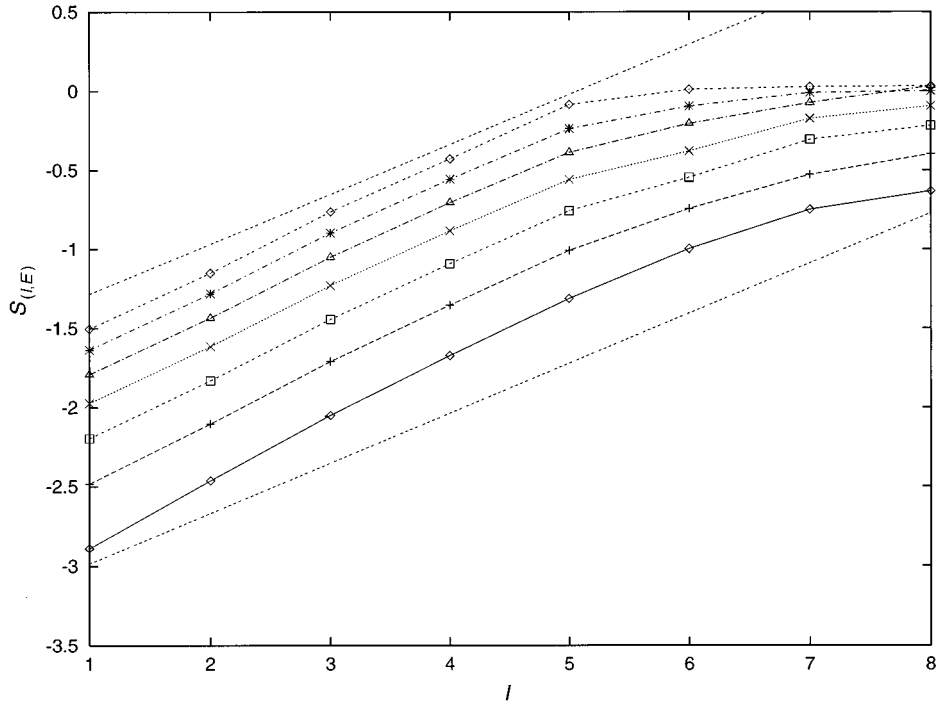

FIG. 7. $S(\tau,\epsilon)$ in Eq. (10) for the Hénon system with 2% dynamical white uniformly distributed noise for different ϵ, $\epsilon=k\times$(noise level), with $k=2-8$. Note that the slopes of the curves differ for different ϵ. For comparison we also plotted the slopes of the clean system (most upper and lower straight lines). Our estimate of the effective (or finite-range) Lyapunov exponent gives approximately 0.4, compared to $\lambda=0.318$ for the Lyapunov exponent of the noise-free system.

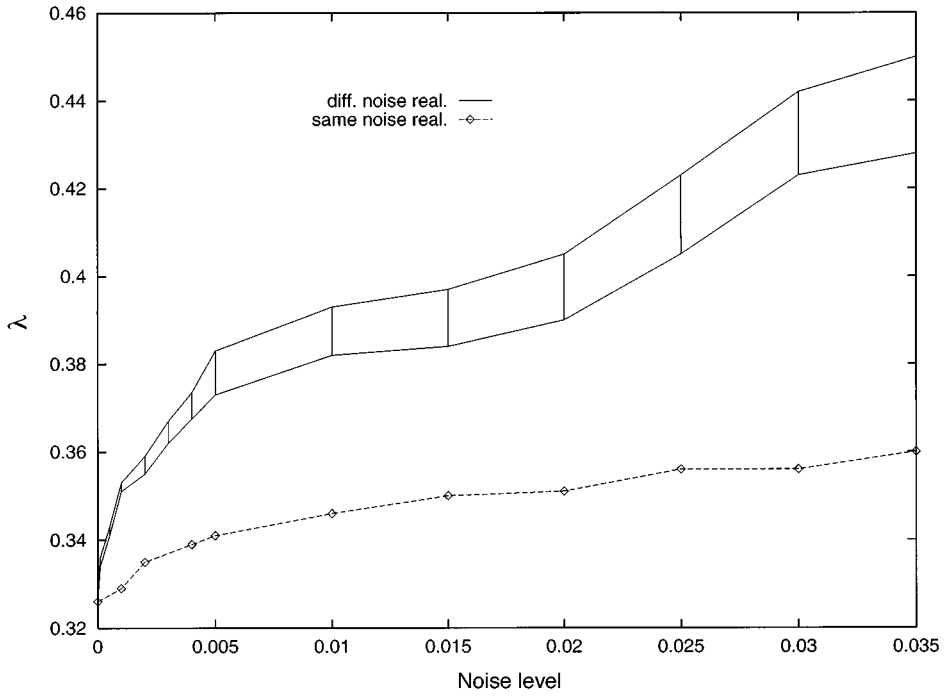

FIG. 8. ''Lyapunov exponents'' for the Hénon system (4) after Eq. (10) (different noise real) and Eq. (8) (identical noise real) for different noise levels. The finite range takes into account the ϵ dependence and curvature effects in curves like Fig. 7.

the phase-space method in [19]. Nevertheless, the notion of Lyapunov exponents becomes awkward in the presence of noise: The clear and unambigious definition of Lyapunov exponents (8) relies on the ability to observe exponential divergence of nearby trajectories in the limit $T\rightarrow\infty$, which implies the limit $\epsilon\rightarrow 0$. This becomes impossible in the presence of noise under different realizations for neighboring trajectories as the initial distance between neighboring trajectories cannot be chosen smaller than the noise level in order to define an exponential divergence. Noise introduces an additional length scale in chaotic systems, below which the divergence of nearby trajectories is dominated by a diffusive process and above which the deterministic divergence occurs. In order to give a measure of the chaos of the noisy system a ''*finite-size Lyapunov exponent*'' [18]

$$\lambda(\epsilon,\Delta n)=\frac{1}{\Delta n}\left\langle \ln\left(\frac{\delta x(n+\Delta n)}{\delta x(n)}\right)\right\rangle \tag{9}$$

along a trajectory $\{x_n\}$ is introduced, where $\delta x(n)=\epsilon$ gives the initial distance between the neighboring trajectories. The average one-step divergence ($\Delta n=1$) measures the predictability of the system with respect to a finite tolerance given a finite initial precision ϵ. In the presence of only one

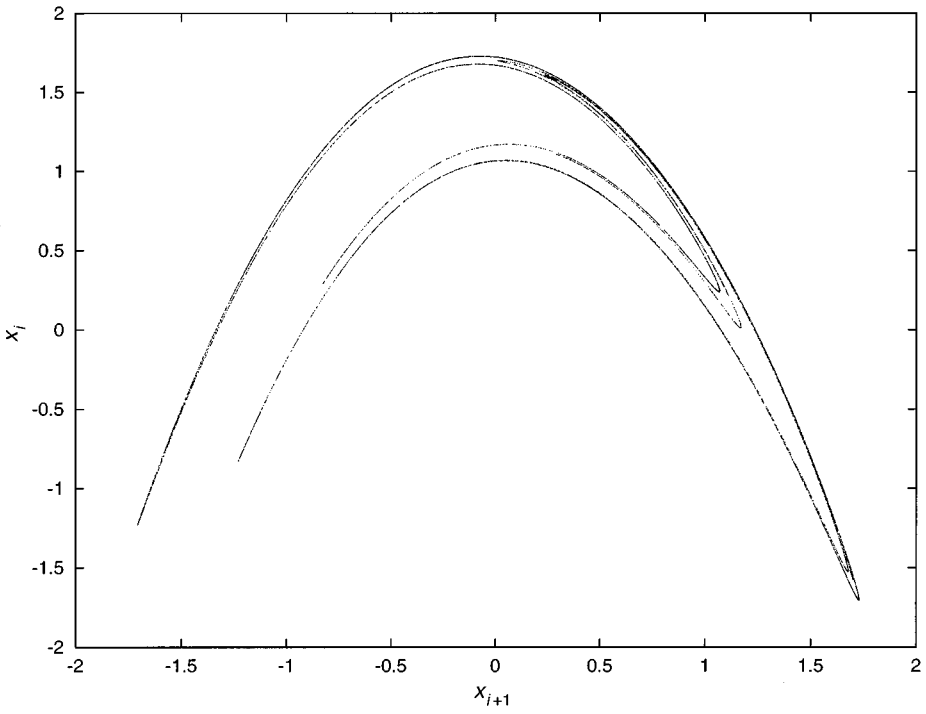

FIG. 9. Attractor obtained by fitting the noisy data underlying Fig. 1 using the cost function (5) with $k=14$ and a function (11) with six neurons.

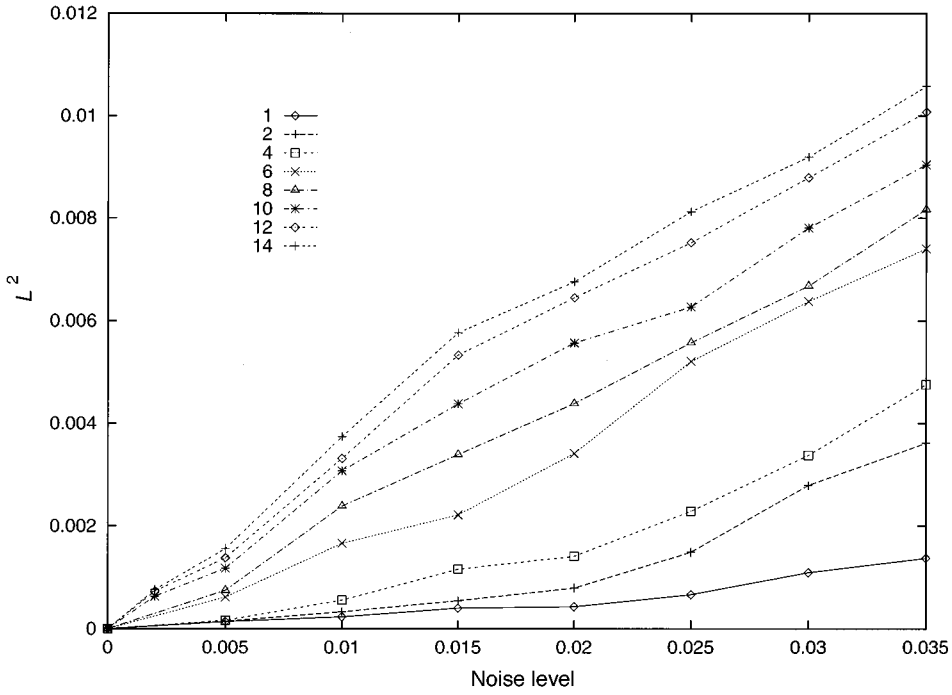

FIG. 10. L^2 distance (12) between the fitted dynamics $\tilde{f}$ and the unperturbed dynamics f as a function of the noise level for the Hénon system (4) for different k used in the construction of $\tilde{f}$ by Eq. (5).

positive Lyapunov exponent this predictability is directly correlated to the ϵ entropy introduced by Kolmogorov [20] and thoroughly discussed in [21]. For $\epsilon \to 0$, $\Delta n \to \infty$ in the noiseless case we recover the usual Lyapunov exponent. But in contrast to the well-defined Lyapunov exponent for infinitesimal perturbations the finite-size Lyapunov exponent is explicit ϵ dependent. In [18] a particular length and time scale are chosen to define a measure of chaos in noisy systems minimizing the information entropy of the noisy system.

The difference of these two different definitions of a Lyapunov exponent (8) and (9) becomes obvious for strongly nonuniform systems where there is an alternation of locally positive and negative Lyapunov exponents over long time periods [18]: In the case of the identical noise realization the contracting intervals can compensate the expanding intervals (as in the noiseless case), and in the case of a corresponding noise-induced shift of the invariant measure a shift from positive to negative values of the Lyapunov exponents can occur [17]. This is no longer possible in the case of different noise realizations: Here for the contracting intervals the contraction is limited to the noise level.

We calculate the finite-size Lyapunov exponent in a modified way using the algorithm to calculate the largest Lyapunov exponent introduced in [22]. This method detects explicitly the exponential divergence of nearby trajectories,

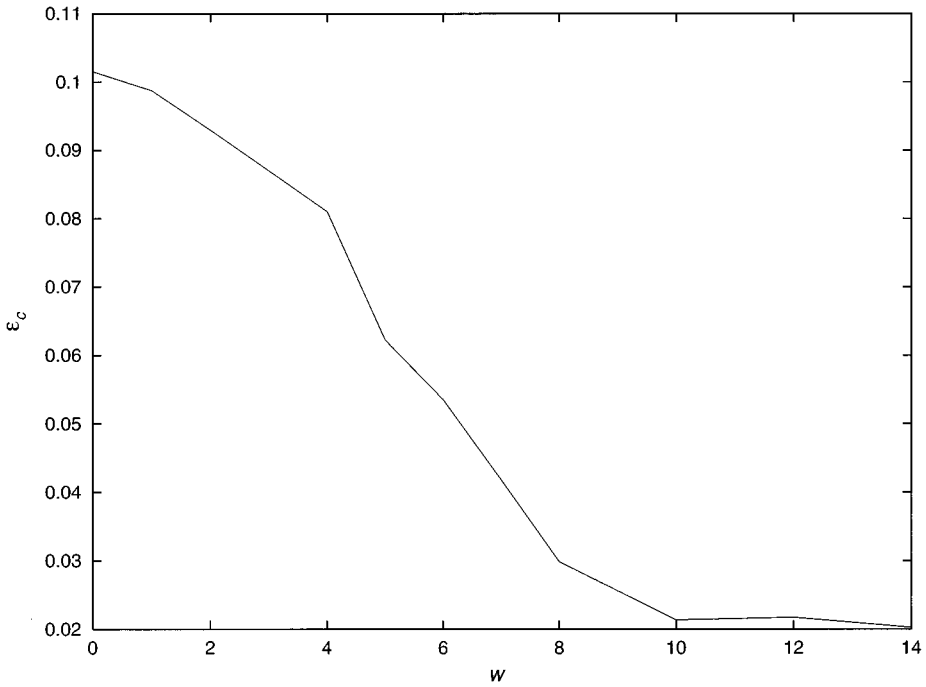

FIG. 11. Geometrical distance ϵ_c defined in Eq. (6) of the attractor of the fitted dynamics from the noisy attractor as a function of k in Eq. (5) for the Hénon system with 3% noise ($n=0$ corresponds to $\tilde{f}=f$).

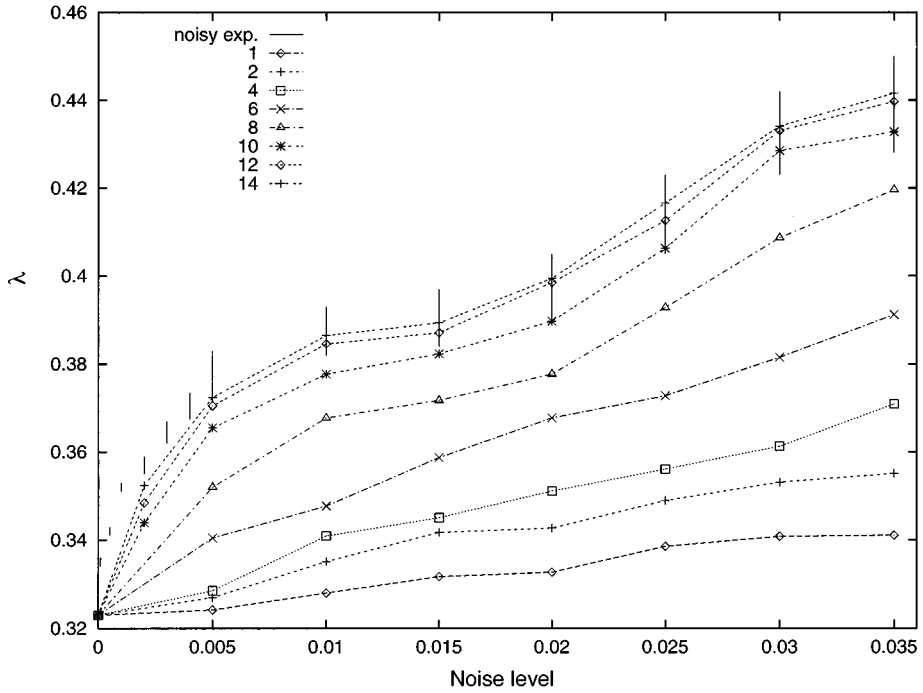

FIG. 12. Lyapunov exponents for the fitted dynamics for different k in Eq. (5) as a function of the noise level. The vertical lines give the results from Fig. 8.

which is implicitly assumed to be the case in [18,19]. Choosing a trajectory of the system of length T, we consider for each point $\mathbf{x}_i$ a certain number K of nearby points $\mathbf{y}_j^i$ that are close to x_i within ϵ. Then we compute the average distances $\mathcal{D}$ between all these neighboring trajectories and the reference trajectories $\{x_i\}$ for the different x_i as a function of the relative time τ. Thus we compute

$$S(\epsilon,\tau)=\frac{1}{T}\sum_{i=1}^{T}\ln\left(\frac{1}{K}\sum_{j=1}^{K}\mathcal{D}(\mathbf{x}_i,\mathbf{y}_i^j;\tau)\right). \tag{10}$$

For a certain range τ, $S(\tau)$ should increase linearly with the slope $\lambda(\epsilon)$, which is the estimate of the Lyapunov exponent. $\partial S(\tau,\epsilon)/\partial\tau$ is equivalent to the average one-step divergence ($\Delta n=1$ and averaging over n) in Eq. (9). For a thorough discussion of this method, see [22]. This scaling is an explicit test for exponential divergence of the trajectories not automatically guaranteed in noisy systems as in addition to exponential divergence of nearby trajectories we have an underlying diffusion process following a power-law behavior. This is shown in Fig. 7, where $S(\tau)$ for the Hénon system with 2% dynamical noise is presented for different ϵ. We clearly observe a scaling range for the growth of the initial perturbation of size ϵ. We also observe that the slope is slightly different for smaller values of ϵ [i.e., $S(\tau)$ is explicitly ϵ dependent]. We stress that for high noise levels the scaling range disappears and an average exponential growth cannot be defined any longer. In Fig. 8 we show the Lyapunov exponents obtained for the two different definitions (8) and (10) for the noisy Hénon system (4) for different noise levels. We explicitly checked for scaling using Eq. (10). The finite bandwidth of the finite-size Lyapunov exponents obtained using Eq. (10) takes into account their ϵ dependence as well as the small curvature. Besides the differences between the two methods, one can clearly observe the deviation from the underlying deterministic system (zero noise).

We claim that the rate of divergence of nearby trajectories under different realizations of the noise is best expressed by the slope in Eq. (10). As we construct effective dynamics for the noisy systems we constructed the cost function (5) such that the change in divergence (change of Lyapunov exponents) due to noise is best considered in the estimate of the optimal model function $\tilde{f}$. Here our focus is on the modeling of these changes. A more systematic investigation about why there occurs a change of the exponential behavior in noisy systems will be explained elsewhere.

V. NUMERICAL INVESTIGATIONS

A. The Hénon attractor

As a numerical illustration we choose the Hénon system (4) with dynamical noise. We will reconstruct the modified features of the noisy system using a modified deterministic model. A construction of an optimally shadowing trajectory with this model will be compared to the construction with the original dynamics.

Constructing an effective dynamics with Eq. (5), we obtain an attractor that shadows the noisy attractor much better than the original attractor. A first impression can be obtained in Fig. 9: Here we show the attractor of the dynamics reconstructed from the data shown in Fig. 1 using the cost function (5) with $k=14$. We intentionally do not restrict ourselves to the structure of the original system in the choice of the *Ansatz* function. Therefore, neural networks [6,23]

$$f(\mathbf{x})=\sum_{i=1}^{6}\frac{a_i}{1+\exp\left(-\sum_{k=1}^{2}w_{ik}x_k-b_i\right)} \tag{11}$$

have proven to yield very good results as a general form of the function f. In particular, we chose a neural net with six neurons in one hidden layer.

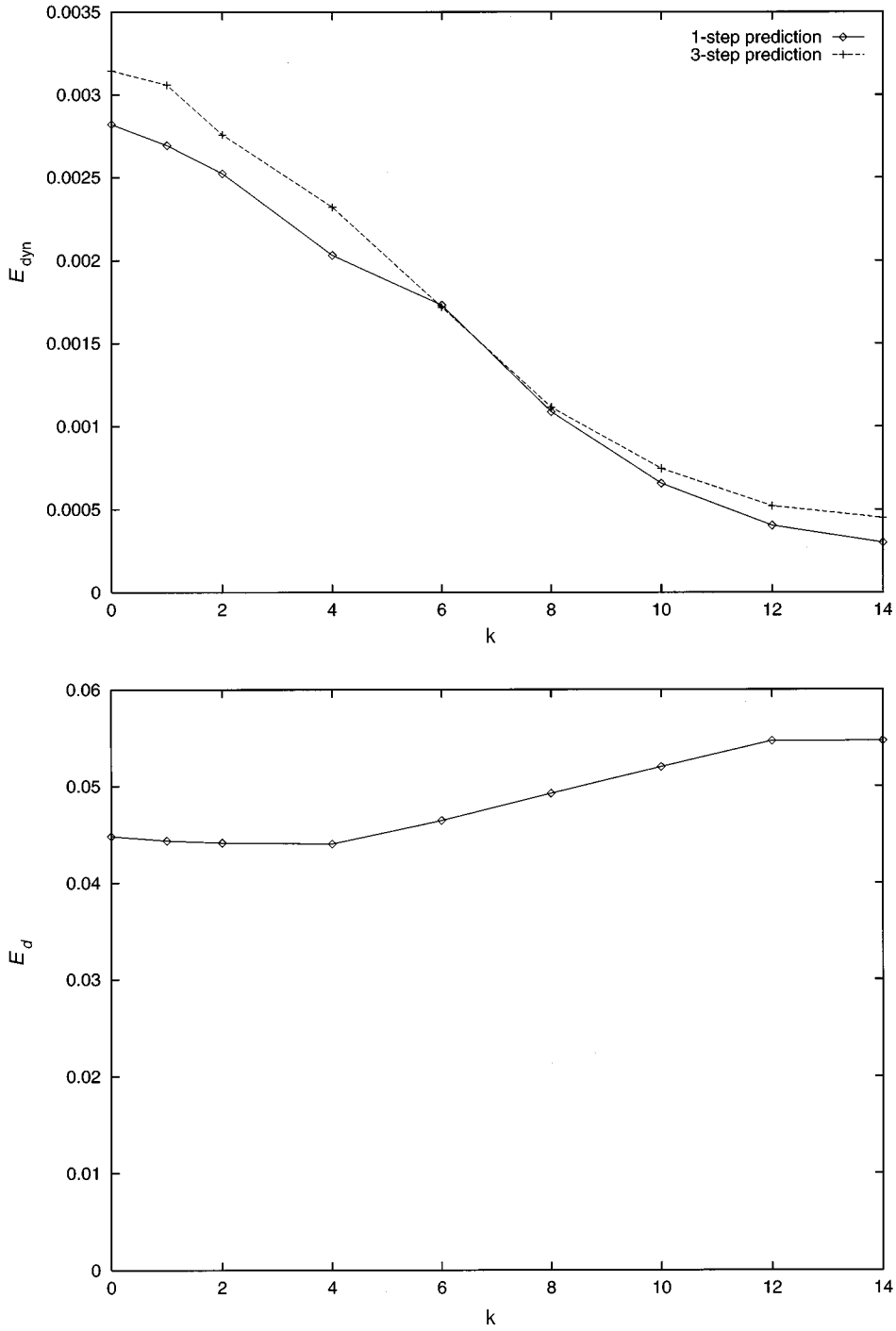

FIG. 13. E^1_{dyn} and E^3_{dyn} (in units of 10^{-1}) for cleaned trajectories dependent on k in the cost function (5) used for the construction of the effective dynamics $\tilde{f}$. The original trajectory was corrupted with 3% noise. The lower panel shows the distance $E_d=[(1/N)\Sigma_i(s_i-y_i)^2]^{1/2}$ of the cleaned from the noisy data ($n=0$ corresponds to $\tilde{f}=f$).

In order to see how the effective dynamics is shifted with respect to the original dynamics [and to compare the effects of varying k in Eq. (5)] we have to introduce a measure for the distances of two dynamical systems. In [6] we introduced a natural form to measure the distance between two maps by the L^2 norm restricted to the attractor $\mathcal{A}$ of the unperturbed dynamics and weighted according to the invariant measure

$$\delta_{L^2}=\langle[f(\mathbf{x})-\tilde{f}(\mathbf{x})]^2\rangle_{\mathcal{A}}\approx\frac{1}{T}\sum_{t=1}^{T}[x_{t+1}-\tilde{f}(\mathbf{x}_t)]^2, \quad (12)$$

where $\{\mathbf{x}_t\}$ is a noise-free time series given by f. This distance is shown in Fig. 10 as a function of the noise level of dynamical noise in the Hénon system using fits as in Eq. (5) for different k. In order to see how much better the effective dynamics obtained with a high step prediction error cost function describes the noisy dynamics we show the attractor distance (ϵ_c for the cross correlation) defined in Eq. (6) in Fig. 11: For high enough k in Eq. (5) the distance to the noisy attractor appears on a scale one order of magnitude smaller than the original dynamics. As impressive are the results for the Lyapunov exponents: In Fig. 12 we show the Lyapunov exponents of the effective dynamics for different k in Eq. (5). They should be compared with Fig. 8 (given by the vertical bars in Fig. 12).

In order to see how much better the ''new'' dynamics describes the noisy data in terms of our concept of pseudo-

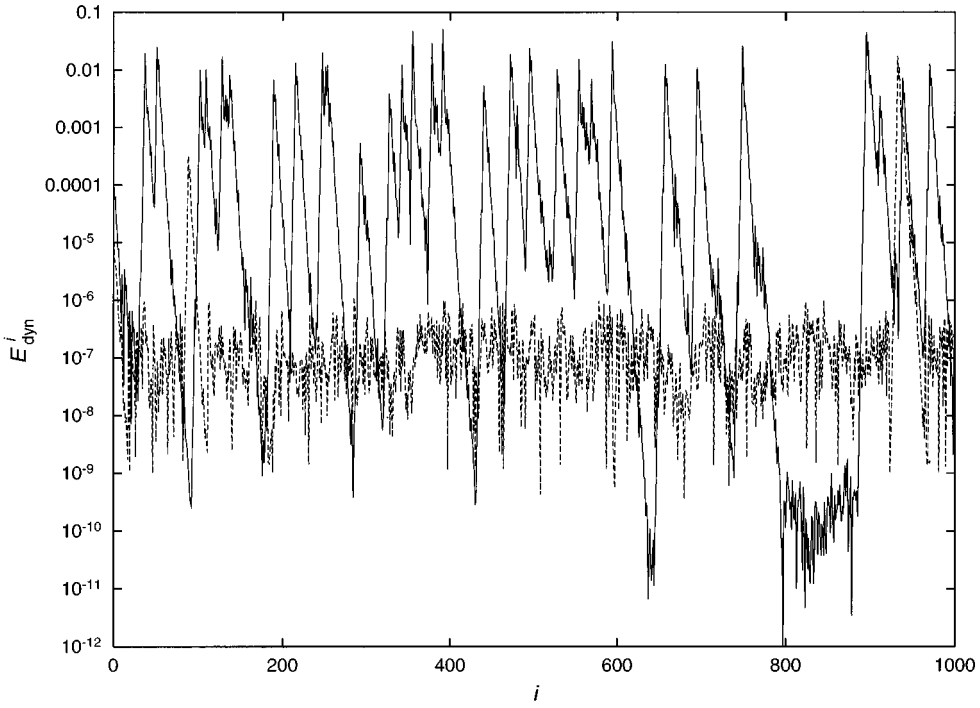

FIG. 14. Individual one-step prediction errors $E^i_{\mathrm{dyn}}=|y_{i+1}-f(\mathbf{y}_i)|$ after noise reduction with Eq. (3) using the original dynamics (Hénon map) and using $\tilde{f}$ of a $k=14$ fit (5) for 3% dynamical noise.

trajectory shadowing, we performed a noise reduction according to Eq. (3) with the original dynamics and the fitted dynamics and calculated the k-step dynamical error

$$E^{(k)}_{\mathrm{dyn}}=\sqrt{\frac{1}{N}\sum_{i=1}^{N}[y_{i+k}-f^k(\mathbf{y}_i)]^2} \tag{13}$$

on the cleaned data $\{y_i\}$. In Fig. 13 we show the result for $k=1$ and $k=3$ for different n-step prediction errors used in the cost function. The values for E^k_{dyn} decrease by an order of magnitude if the multistep prediction error in Eq. (5) is used in the fits. In Fig. 14 we show the individual E^i_{dyn} after noise reduction for the original dynamics and $\tilde{f}$ (compare also Fig. 2).

All these figures show very well how much better the noisy system can be described by the modified dynamics. Figures 9–12 together give a very nice example of the possibility of describing noisy systems by modified effective dynamics: (i) The constructed cleaned trajectory is more deterministic (i.e., with lower E_{dyn}) than the equivalent one for the original dynamics, (ii) the synthetic attractor describes the geometric features of the noisy attractor much better, and (iii) the quantitative analysis of Lyapunov exponents indicates that features of the noisy system are better described by the modified dynamics.

B. An experimental example

As a further example of the effect of the noise-induced attractor deformation and our finding of an effective dynamics we want to illustrate our method for an experimental data set. Figure 15(a) shows the attractor of a Poincaré map of the laser experiment with feedback, run by the National Institute of Optics in Florence, Italy [24]. It was calculated by a fit with a neural network with six neurons. We artificially perturbed the map with 1% white, uniformly distributed noise. The resulting noisy attractor is shown in Fig. 15(b). We can clearly observe the attractor deformation at homoclinic tangencies [which are also marked in Fig. 15(a), calculated after the method in [8]]. In Fig. 15(d) we show a part of the obtained attractor performing a fit using the cost function (5) with $k=12$. This gives a deterministic attractor much better serving as a skeleton for the noisy attractor in Fig. 15(b) [with the same part as in Fig. 15(d), given also in Fig. 15(c)]. We want to make one brief comment about the origin of noise in the surface of sections of experimental flows. Noisy flows do not reduce to noisy maps in the way we have treated them. In general, the noise will depend on the point in the surface of section [8]. The effect of noise is different in different parts of the phase space, depending on the local stretching and dissipation resulting in a spatially dependent amplitude density of noise in the Poincaré section. But the general effect of the noise-induced attractor deformation appears as well. An investigation on experimental systems with dynamical noise is in progress [25].

VI. CONCLUSION

We presented a different approach to characterize data that are contaminated by dynamical noise. This method is based on the idea of a modified shadowing in nonhyperbolic systems: parameter shadowing. The features of the noisy system can be quite different from the underlying deterministic system, which is (i) geometrically expressed in attractor modifications [8], which leads to different scaling behavior for the correlation dimension expressed by a large deviation from the original attractor in the cross correlation integral, and (ii) quantitatively expressed in different values of the finite-range Lyapunov exponents $\lambda(\epsilon)$ for the noisy system. We were able to show how much better the noisy system can be described by a modified dynamics (i) leading to an attractor with geometrical features similar to the noisy system and (ii) yielding values of λ that are similar to the noisy system.

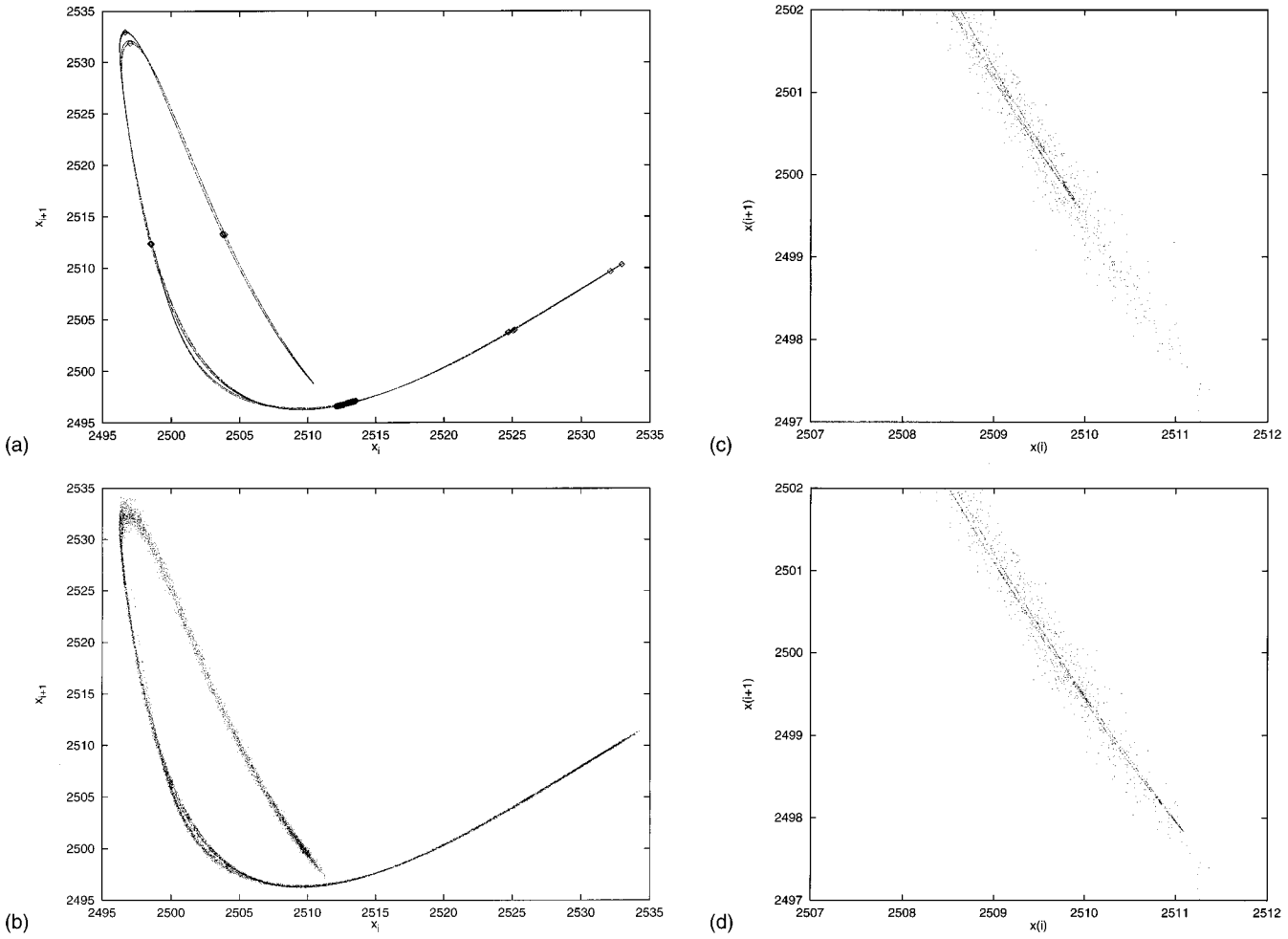

FIG. 15. (a) Poincaré map of the Florence Laser attractor with homoclinic tangencies. (b) Attractor with dynamical noise. (c) Enlargement of a noisy attractor (b) and the attractor in (a). (d) Enlargement of a noisy attractor (c) and the attractor of a dynamics obtained by a fit (5) with $k=12$.

Our method of constructing this effective dynamics $\tilde{f}$ is based on using a multistep prediction error in the cost function (5) such that locally shadowing pieces of trajectories are constructed and the dynamics $\tilde{f}$ underlying these shadowing trajectories can be extracted. With the help of $\tilde{f}$ a less noisy trajectory can be constructed using methods introduced in [1,4,5]. It remains an open problem whether an exactly shadowing trajectory for a modified dynamics exists generally for nonhyperbolic systems in the sense of the ordinary shadowing theorem [7] for hyperbolic systems (as was shown for very specific one-dimensional maps in [9]). This question exceeds the purpose of this paper, but we hope to be able to give some qualitative reasoning in this direction.

Our last point concerns the analysis of real data: Dynamical noise evidently is present in many physical data sets. Often the detection of dynamical noise remains impossible (see [26]). Our cost function (5) should give some hints in this directions (if the observed noise level is not too high): If we use different k and obtain varying results for the fit (consistently for different forms of the *Ansatz* f_p) we can give evidence of the presence of dynamical noise. On applying the standard techniques of nonlinear time-series analysis one most likely obtains results corresponding to the modified, effective dynamics rather than the original dynamics.

[1] C. Grebogi, St. Hammel, J. Yorke, and T. Sauer, Phys. Rev. Lett. **65**, 1527 (1990); S. M. Hammel, J. M. Yorke, and C. Grebogi, J. Compl. **3**, 136 (1987).
[2] J. C. Sommerer, E. Ott, and C. Grebogi, Phys. Rev. A **43**, 1754 (1991).
[3] P. Grassberger, R. Hegger, H. Kantz, C. Schaffrath, and T. Schreiber, CHAOS **3**, 127 (1993).
[4] J. D. Farmer and J. J. Sidorowich, Physica D **47**, 373 (1991).
[5] M. Davies, Int. J. Bifurc. Chaos **3**, 113 (1992); M. Davies, Physica D **79**, 174 (1994).
[6] L. Jaeger and H. Kantz, CHAOS **6**, 440 (1996); H. Kantz and L. Jaeger, Physica D (to be published).
[7] For an excellent overview, see R. Bowen, *On Axiom A systems*, CBMS Regional Conference Series in Mathematics Vol.

35 (American Mathematical Society, Providence, RI, 1970); B. V. Anosov, Proc. Steklov Inst. Math. **90**, 1 (1967); R. Bowen, J. Diff. Eq. **18**, 333 (1975).
[8] L. Jaeger and H. Kantz, Physica D (to be published).
[9] H. E. Nusse and J. A. Yorke, Commun. Math. Phys. **114**, 363 (1988).
[10] T. Sauer, J. Yorke, and M. Casdagli, J. Stat. Phys. **65**, 579 (1991).
[11] M. Hénon, Commun. Math. Phys. **50**, 69 (1976).
[12] P. Grassberger, H. Kantz, and U. Mönig, Phys. Lett. **113A**, 235 (1985); J. Phys. A **22**, 5217 (1989).
[13] P. Grassberger and I. Procaccia, Phys. Rev. Lett. **50**, 346 (1983); Physica D **9**, 189 (1983).
[14] H. Kantz, Phys. Rev. E **49**, 5091 (1994).
[15] Y. Kifer, *Theory of Random Transformations* (Birkhäuser, Boston, 1986).
[16] L. Arnold, in *Dynamical Systems*, edited by R. Johnson, Lecture Notes in Mathematics Vol. 1609 (Springer, Berlin, 1995).
[17] A. Maritan and J. R. Banavar, Phys. Rev. Lett. **72**, 1451 (1994); G. Malescio, Phys. Lett. A **218**, 25 (1996).
[18] V. Loreto, G. Paladin, and A. Vulpiani, Phys. Rev. E **53**, 2087 (1996); G. Paladin, M. Serva, and A. Vulpiani, Phys. Rev. Lett. **74**, 66 (1995).
[19] A. Wolf, J. B. Swift, H. L. Swinney, and J. A. Vastano, Physica D **16**, 285 (1985).
[20] A. N. Kolmogorov, IRE Trans. Inf. Theory **1**, 102 (1956).
[21] P. Gaspard and X. J. Wang, Phys. Rep. **235**, 291 (1993).
[22] H. Kantz, Phys. Lett. A **185**, 77 (1994).
[23] R. Gencay and W. D. Dechert, Physica D **59**, 142 (1992).
[24] F.T. Arecchi, W. Gadomski, and R. Meucci, Phys. Rev. A **34**, 1617 (1985); M. Ciofini, R. Meucci, and F.T. Arecchi, Phys. Rev. E **52**, 94 (1995).
[25] L. Jaeger, H. Kantz, R. Hegger, H. Beige, and M. Diestelhorst (unpublished).
[26] G. D. Szpiro, Physica D **65**, 289 (1993).